

# Air Flow Measurements During Medium-Voltage Load Current Interruptions

Nina Sasaki Støa-Aanensen<sup>1,2</sup>, Magne Runde.<sup>2</sup>

<sup>1</sup>Norwegian University of Science and Technology, Trondheim 7491, Norway, [nina.aanensen@ntnu.no](mailto:nina.aanensen@ntnu.no)

<sup>2</sup>SINTEF Energy Research, Trondheim 7465, Norway

Air has been considered a good alternative to SF<sub>6</sub> as arc quenching medium for load break switchgear at medium voltage ratings. In this work, the air flow characteristics and influence from the electric arc have been studied for typical currents and over-pressures. The cooling air velocity is typically in the range 150 - 200 m/s and thus well below supersonic speed. The arc and the surrounding hot air severely affect the air flow pattern by causing clogging in the contact and nozzle region.

**Keywords:** Load break switch, switchgear, medium voltage, arc, air flow, thermal interruption.

## 1 INTRODUCTION

Reducing the use of sulfur hexafluoride (SF<sub>6</sub>) in high voltage apparatus will in the long term lower the emissions of this strong "greenhouse gas" to the atmosphere. Air may be a good alternative to SF<sub>6</sub> as arc quenching medium for switchgear with modest ratings, e.g., medium voltage (MV) load break switches (LBSs). These often use a gas flow to cool and quench the arc, have a typical interrupting capability up to 630 A, and are installed in 6 - 36 kV systems.

An extensive on-going investigation examines how the various design features (contact and nozzle geometries, air flow) of a simple MV air LBS affect its interrupting capability under different conditions (current amplitude, steepness of recovery voltage) [1] - [3]. As expected, the air flow, or more precisely, the upstream over-pressure producing the air flow onto the arc, is found to be of crucial importance.

The present paper takes a closer look at the air flow characteristics during contact separation and current interruption in this simple switch, by using a Venturi tube and pressure sensors installed near the nozzle and contacts. In particular, it is of interest to obtain quantitative information about the air velocity and mass flow rates, and to determine to what extent the arc obstructs or clogs the flow.

## 2 EXPERIMENTAL SETUP

The test switch and pressure measurement set-up is shown in Fig. 1. A 10-liter pressure tank (to the left) is used to generate the air flow during the contact opening and current interruption process. The moving pin contact (to the right) has a starting position well inside the tulip contact. Together with an o-ring, the pin contact acts as a plug for the tank opening, so that the air in the tank can be pre-set to an over-pressure before the interruption test starts.

In closed position current flows through the tank wall via the tulip contact and over to the pin contact, which is connected to the load side of the circuit. By releasing a compressed spring, the pin contact is pulled out from the tulip contact, at a speed of  $5 \pm 0.5$  m/s.

Pressure sensors are installed at each end of a Venturi tube (positions 1 and 2). The Venturi tube guides the air flow so that the air velocity can be determined from the pressure drop between 1 and 2. The pressure sensors are of type Kistler 4260A with a frequency response of 2 kHz and an accuracy of 0.005 bar. The sampling frequency was 5 kHz.

If the over-pressure in the tank provides sufficient air flow and cooling of the arc, the current is interrupted at current zero (CZ). If not, the current continues to flow until the next CZ. The test switch has two or three such attempts, before the current is cleared by the laboratory circuit breaker.

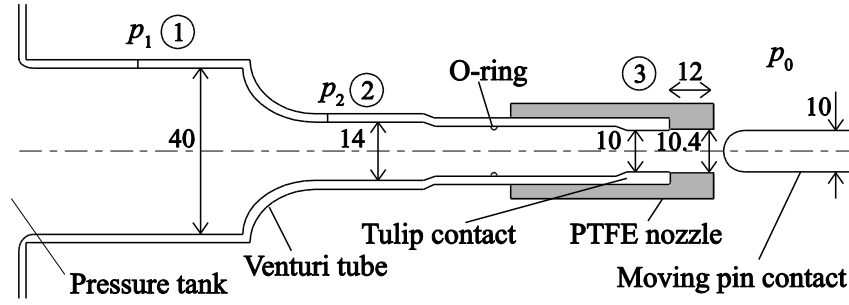


Fig. 1. The test switch setup. A venturi tube is connected between a pressure tank and a copper-tungsten tulip contact. At the right hand side of the tulip contact and a cylindrical PTFE nozzle, air is at atmospheric pressure,  $p_0$ . All dimensions are in millimeters.

A near-infrared high-speed camera (Cheetah 1470, Xeneth) captured images of the arc during interruption. The integration time is  $3.7 \mu\text{s}$ . In addition, current, voltage across the contact gap, and contact position are recorded.

Both the current and the transient recovery voltage (TRV) can be adjusted and controlled. More details about the laboratory setup and test circuit settings are given elsewhere [2], [4].

### 3 AIR VELOCITIES AND MASS FLOW RATES

Initial pressure measurements were carried out during dry switching operations, i.e., without current and arc. Fig. 2 shows the pressure drops between position 1 and 2 for pre-set tank over-pressures in the range 0.1 - 0.4 bar, which are typical values for the considered switch design and ratings. As can be seen from the curves, the noise level of the measurements is in excess of 0.01 bar.

The pressure difference before contact separation is approximately zero, indicating no air flow. After separation, the pressure difference increases to a level determined by the initial tank pressure, before it starts decaying after around 20 ms. As expected, the higher the initial over-pressure in the tank, the higher the pressure drop after contact separation, yielding increased air velocity and a higher mass flow rate.

With basis in the pressure measurements, more details about the air flow can be deduced. Using a numerical software package [5] the mass flow rate and air velocity at position 2 have been calculated, assuming ideal

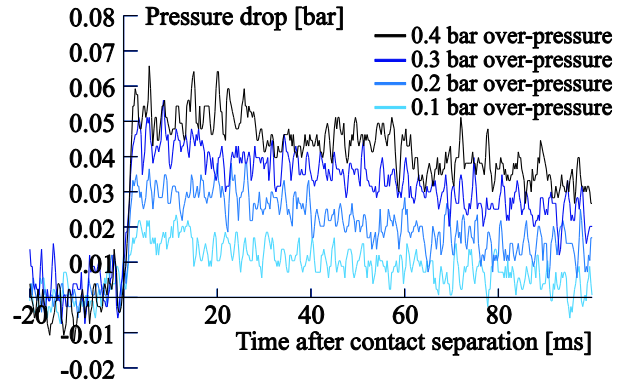


Fig. 2. Measured pressure drop between position 1 and 2 during contact separation (no current). The pre-set over-pressures in the tank before contact opening are indicated.

gas and including a standard k- $\epsilon$  turbulence model. Furthermore, the air velocity through the tulip contact (position 3 in Fig. 1) is also calculated.

As a simpler and presumably far less accurate alternative, the air velocity and mass flow rate can be estimated solely from the initial over-pressure, assuming an incompressible inviscid flow:

$$v_3^* = \sqrt{\frac{2p_1}{\rho}}, \dot{m}_3^* = \rho A v_3^*, \quad (1)$$

deduced from the well-known Bernoulli equation. Here, the mass density of air,  $\rho$ , is assumed constant and equal to  $1.225 \text{ kg/m}^3$  (the value at standard atmosphere), and  $A$  is the tulip contact inner cross sectional area.

Table 1 lists the measured pressure values 5 - 15 ms after contact separation, together with the air velocities and mass flow rates at position 3 determined by both methods.

*Table 1. Measured pressures and estimated air velocities and mass flow rate; tulip contact inner diameter is 10 mm.*

Measured pressures		Numerical calculation		Bernoulli, Incompr.	
$p_1$ [bar]	$p_2$ [bar]	$\dot{m}_3$ [kg/s]	$v_3$ [m/s]	$\dot{m}_3^*$ [kg/s]	$v_3^*$ [m/s]
0.40	0.345	0.019	180-190	0.025	256
0.30	0.255	0.016	150-160	0.021	221
0.20	0.170	0.013	130-140	0.017	181
0.10	0.085	0.009	90-100	0.012	128

With a tulip contact diameter of 10 mm, which is a typical dimension for MV LBSs, an over-pressure of 0.1 - 0.4 bar corresponds to an air flow velocity in the range of 100 - 200 m/s, and a mass flow rate of 0.01 - 0.02 kg/s. The simpler approach based on the Bernoulli equation over-estimates the air velocity and mass flow rate by some 30 - 50%.

According to Eq. (1), the air velocity does not depend on the diameter of the tulip contact, but the mass flow rate does. Hence, a smaller tulip contact inner diameter (a smaller tank outlet) is expected to give the same air velocity for a certain over-pressure.

In order to check the validity of this assumption, the pressures at position 1 and 2 have been measured with a tulip contact of diameter 7.1 mm. However, by using such a narrower tank outlet, the pressure drop becomes smaller due to the decreased mass flow rate. This results in less accurate measurements, as the pressure differences approach the sensitivity of the measuring system. Still, pressure measurements obtained with 0.3 and 0.4 bar over-pressures have been used as input for numerical calculations of the air velocity through a 7.1 mm wide tulip contact. These are presented in Table 2, together with the resulting mass flow rates and the corresponding estimates based on Eq. (1).

Tables 1 and 2 show that the air velocities found by numerical calculations for 10 and 7.1 mm tulip contact inner diameters are fairly similar. This supports the assumption that the

air velocity for practical purposes here is determined by the over-pressure in the tank, and not by the tulip contact dimensions. The mass flow rate, in contrast, becomes significantly lower, as expected.

An over-pressure of 0.4 bar was found sufficient for interrupting currents up to approximately 800 A with a TRV corresponding to the thermal phase of the 24 kV "mainly active load" test duty [6]. The corresponding air velocity is well below the speed of sound, making the entire concept of current interruption at MV LBS ratings significantly different from that of high voltage circuit breakers, where supersonic gas flow is common.

*Table 2. Measured pressures and estimated air velocities and mass flow rates; tulip contact inner diameter is 7.1 mm.*

Measured pressures		Numerical calculation		Bernoulli, Incompr.	
$p_1$ [bar]	$p_2$ [bar]	$\dot{m}_3$ [kg/s]	$v_3$ [m/s]	$\dot{m}_3^*$ [kg/s]	$v_3^*$ [m/s]
0.40	0.385	0.010	190-200	0.012	256
0.30	0.290	0.008	150-160	0.011	221

#### 4 ARC INFLUENCE ON AIR FLOW

This section investigates to what extent the arc affects the air flow. Fig. 3 shows pressure measurements at positions 1 and 2 during a successful 880 A current interruption test. The magnetic field generated by the current flowing through the Venturi tube wall caused a 50 Hz disturbance up to the point of current interruption, approximately 3 ms after contact separation. This has been manually removed. A plot showing the pressure drop is also included in the bottom part of the figure.

Fig. 4 contains similar plots of pressure drops as a function of time for six different interruption tests. In all the tests the current was 880 A, but the pre-set tank over-pressure varied from 0.2 bar to 0.4 bar. A pressure drop measurement without current is included in each plot for comparison

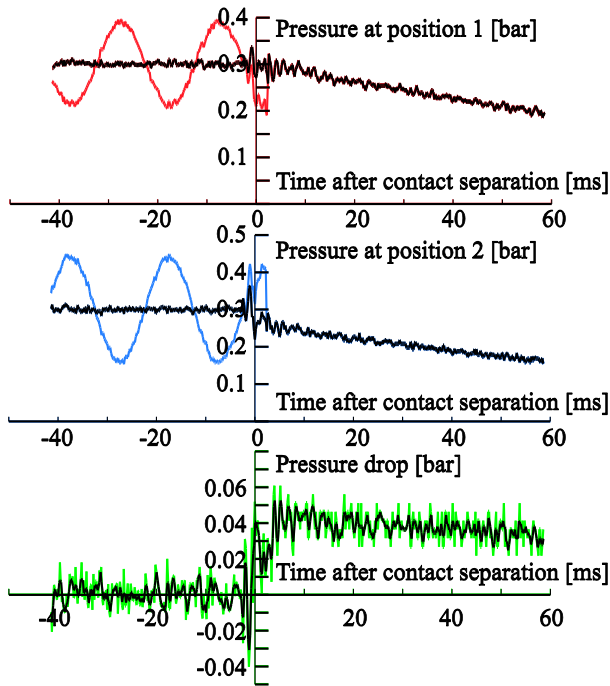


Fig. 3. Pressure measured at position 1 (red line, upper plot) and position 2 (blue line, middle plot) during a 880-A current interruption test. In the black lines, the 50 Hz disturbance has been removed. The lower plot shows  $p_1 - p_2$  (green) and its corresponding three-point running average (black).

Both interruption tests in the 0.4-bar plot were successful, having approximately the same arcing time of 8 - 9 ms. The transition from zero to approximately 0.055 bar pressure drop comes later than in the case without current. The delay corresponds to the arcing time, suggesting that the arc at least partly clogs the air flow. After the arc is extinguished, the pressure drop reaches the same level in all three cases.

In the middle plot of Fig. 4, one test interrupted at first CZ, which occurred immediately after contact separation. The other failed at first attempt, but interrupted successfully at its second CZ. As in the 0.4-bar case, the two pressure drop curves are clearly linked to the arcing. In the test failing to interrupt at first CZ, the pressure difference appears to increase also around this first attempt, and not only after the successful interruption. This may be explained by that the arc cross section is small near CZ, and to a lesser extent clogs the air flow (even if the interruption fails).

The pressure curves in the lower plot can be

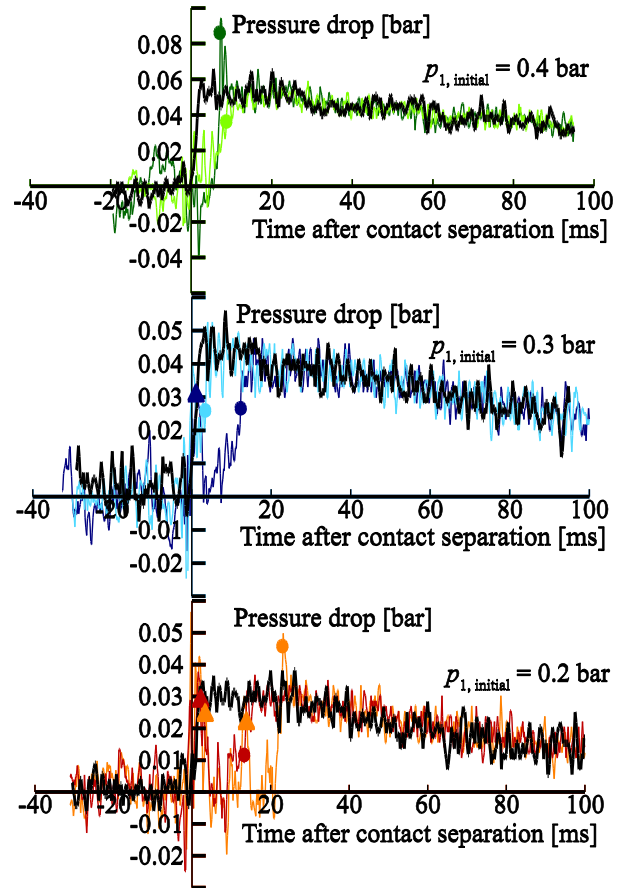


Fig. 4. Measured pressure drops between position 1 and 2 during opening operations with (colored) and without (black) current, and with different pre-set over-pressures. The filled circles in the plot indicate successful interruptions and triangles are interruption attempts that failed.

interpreted in a similar manner. As long as an arc is burning between the contacts, it considerably influences the air flow by clogging the nozzle and contact gap, especially around the high-current part of the half-cycle. After the arc has been extinguished, the pressure drop increases to the same level as in the dry switching case.

The plots in Fig. 4 indicate that an 880-A arc is large enough to cause clogging of a channel with a 10 mm diameter. According to [7] and [8], an 880-A arc can be expected to have a diameter in the range 2.6 - 4.8 mm. This is less than half of the nozzle inner diameter, and thus only a small fraction of the channel. However, the moving arc causes heating and expansion of the surrounding air, and this may also contribute to the clogging.

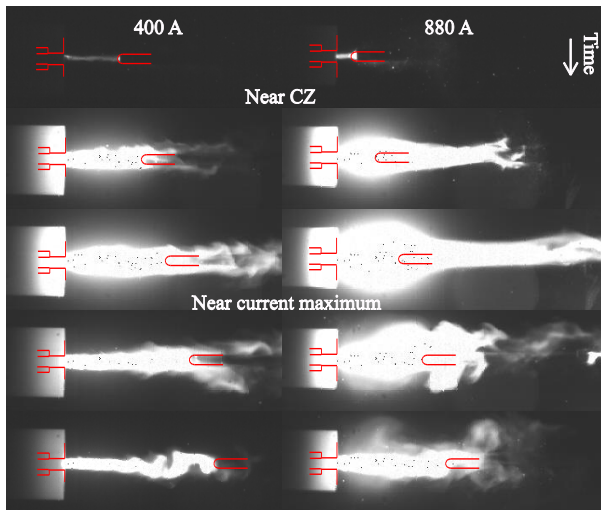


Fig. 5. Comparison of arc and surrounding hot gas with currents of 400 A and 880 A for the second half-cycle after contact separation. The tulip and pin contact diameters are 7.1 mm, and the nozzle is 12 mm long with an inner diameter of 7.4 mm. The contour of the pin contact and inner part of tulip contact and nozzle are drawn onto the images. The time between each frame is approximately 2.8 ms.

In similar experiments with currents of 400 A and 630 A, the same was observed; long arcing times led to clogging of the air flow. The diameters of 400-A and 630-A arcs are estimated to 1.8 - 3.2 mm and 2.2 - 4.0 mm, respectively [7], [8], again small compared to the nozzle inner diameter.

In the experiments reported here, a large pressure tank was used as reservoir for the cooling air, and the arc did not cause any observable pressure rise in the tank. This is different from a typical commercial puffer-based device, where the gas reservoir is much smaller and clogging is likely to increase the upstream pressure. This could lead to an even greater effect of the arc on the gas flow and cooling than in the present setup. Thus, the influence of the arc on the gas flow pattern is a crucial factor that must be taken into account when designing puffer devices, also for MV LBS ratings, where currents and arc cross-sections are rather small.

Fig. 5 shows images recorded during two interruption tests with 400-A and 880-A currents. As can be seen, the near-infrared camera not only captures the arc, but also the sur-

rounding hot air. This makes it difficult to estimate the size of the arc. Still, there is a clearly observable difference between the two currents, with a lot more hot gas surrounding the arc channel and to the right of the pin contact tip in the 880-A case. The arc and hot gas region extend radially well beyond the tulip contact and nozzle inner diameters, and it seems reasonable that the arc is able to cause clogging during the high current part of the half-cycle.

## 5 CONCLUSIONS

Upstream pressures of 0.3 - 0.4 bars have in earlier work been found to generate air flows that are sufficient to interrupt load currents in a typical MV switch design. In the present work a study of the air flow and its interaction with the arc shows that:

- The air velocity is in the range 150 - 200 m/s and thus well below supersonic speed. Consequently, the arc cooling and current interruption process is here quite different from that of high voltage circuit breakers, where the gas flow normally is supersonic.
- The arc and the surrounding hot air severely affect the air flow pattern by causing clogging in the contact and nozzle region. Thus, it is important to consider the effects of clogging when designing MV LBSs.

### Acknowledgements

This work is supported by the Norwegian Research Council.

### REFERENCES

- [1] Jonsson E, Aanensen N S, Runde M, IEEE Trans Power Del, 29 no. 2 (2014), 870 - 875.
- [2] Aanensen N S, Jonsson E, Runde M, IEEE Trans. Power Del., 30 no. 1 (2015), 299 - 306.
- [3] Jonsson E, Runde M, IEEE Trans Power Del 30 no. 1 (2015), 161 - 166.
- [4] Jonsson E, Runde M, In: Proc. Int. Conf. Power Systems Transients, Vancouver, 2013.
- [5] ANSYS FLUENT, release 13.0 ANSYS Inc, 2010.
- [6] Støa-Aanensen N S, Runde M, Jonsson E, Teigset A D, submitted to IEEE Trans Power Del, 2015.
- [7] Ramakrishnan S, Rogozinski M W, J Phys D: Appl Phys 30 (1997), 636 - 644.
- [8] Lowke J J, Ludwig H C, J Appl Phys 46 (1975) 3352 - 3360.